SINGLE BEAM INTERFEROMETRY OF A THERMAL BUMP: I -EXPERIMENT

P.K. Kuo and M. Munidasa

Department of Physics
Wayne State University
Detroit, MI 48202

INTRODUCTION

We present a sensitive interferometric technique which simultaneously measures the optical, elastic and thermal parameters of solids. We obtain the optical reflectivity change and the displacement due to thermal expansion (thermal bump) produced by an intensity modulated and focused laser beam.

In this scheme a probe beam larger than the size of the thermal bump is reflected from the sample surface. Earlier works [1] have used a probe beam smaller than the size of the thermal bump. The information is contained in the distortion of the reflected wave-front, caused by the thermal bump. This information about the material properties is obtained by measuring the interference pattern produced by the superposition of the distorted ac wave-front from the bump and the reflected undistorted dc wave-front from the surrounding surface (Figure 1). Interference patterns of this type has been observed before [2] in the reflected laser beam from a liquid surface. The interference pattern is measured by scanning a photo-detector across the reflected probe beam. Since only a single beam is used, noise from mechanical vibrations and fluctuations in air currents are greatly reduced. The signal is detected synchronously with the modulation of the thermal bump, using a lock-in amplifier. Experimental data are fitted to a phenomenological theory using a multi-parameter least-squares fit routine. Optical and thermal parameters are deduced from these fits.

EXPERIMENTAL METHOD

Figure 2 depicts the experimental arrangement used. The heating beam is obtained from the 4880 Å line of an Argon ion laser, intensity-modulated by means of an acousto-optic modulator, and subsequently focused to a ~10 μm spot on the sample surface. The average incident power is about 40 mW. The 6328 Å beam from a 3 mW He-Ne laser is used as the probe beam. This beam is not focused, and has a spot diameter of about 800 μm at the sample. The heating beam spot can be laterally displaced with respect to the center of the probe beam spot by moving the focusing lens. The probe beam reflected from the sample surface is detected by a photodiode with a slit (width of ~50 μm) in front of it. The photodiode (without the slit) is large enough to capture the entire probe beam. The detector/slit assembly is scanned across the beam using a stepping-motor-driven scanning stage to record the interference pattern. The signal is synchronously detected by a lock-in amplifier. The data are collected by a micro-computer which also controls the stepping motor.

A detailed knowledge of the probe beam's characteristics is essential in the quantitative analysis of the data. The position and magnitude of the Gaussian beam waist are separately determined by measuring the beam profile at several distances on the same setup with a chopped probe beam.

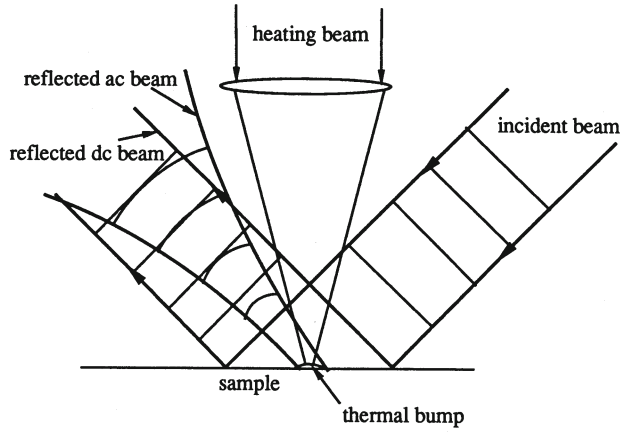

Fig. 1. Wave front figure of the incident and the reflected probe beam.

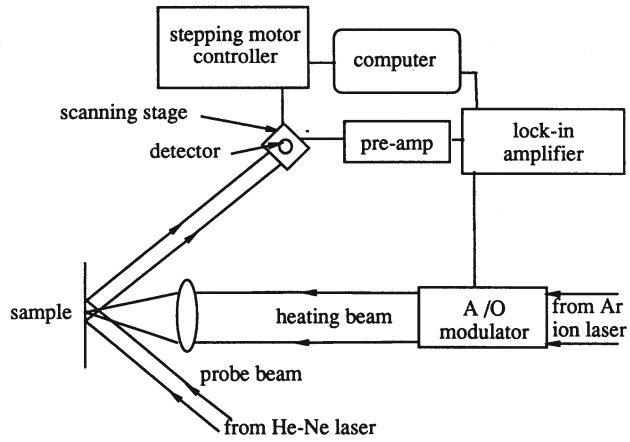

Fig. 2. Experimental arrangement.

Using our interferometer on a silicon wafer we are at present able to get a usable signal (with a 1-second time constant) with a heating beam power as low as 0.1 mW (Figure 3). This corresponds to a bump height of ~ 10^{-3} Å at 1 kHz. We have not yet achieved sensitivities reported by other interferometric techniques.[3-5] Those techniques, however, use much more elaborate experimental arrangements than that described here.

PHENOMENOLOGICAL THEORY

The interference between spherical (from the bump) and a planar wavefronts (from the surrounding surface) gives rise to the traditional pattern of Newton's rings. Due to the small size of both the thermal bump and the probe beam, only two or three of the rings are visible at an experimentally convenient distance. To obtain quantitative information from such an interference pattern, the traditional fringe counting method would be too imprecise. Ideally one would want to do a least-square fit of the measured data to a theoretical calculation of the fringe pattern based on the detailed shape and time variation of the thermal bump. Such a calculation from first principles is being undertaken by Favro and Munidasa [6]. In this report we present a more heuristic approach to the analysis of acquired data.

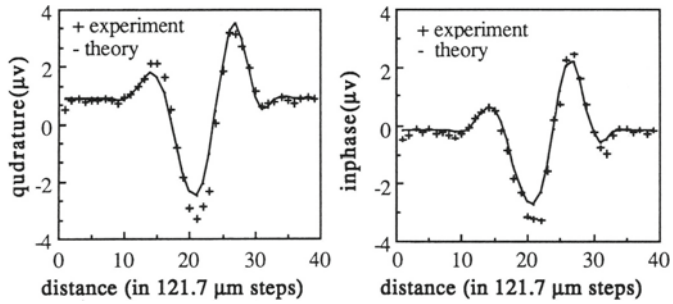

Fig. 3. Experimental data and theoretical fit of inphase and qudrature signal for a Si wafe with a heating beam power of 0.1 mW and a modulation frequency of 1 kHz. Bump height calculated from the fit is 3 x 10^{-3} Å.

We make a simplifying assumption that the height of the thermal bump has a Gaussian shape and that the entire bump has a spatially uniform phase which follows the modulated heating beam. Accordingly we express this height as

$$h\,(x,y,t) \;=\; \delta h \cos\,(\Omega t + \theta_h)\, \exp\,[-(x^2+y^2)/r_b^2] \quad , \tag{1}$$

where δh is the amplitude, θ_h is the phase and r_b is the Gaussian radius of the bump. The (angular) frequency of the heating modulation is Ω. These assumptions are somewhat arbitrary for the general situation, but they are quite reasonable in cases for which the thermal diffusion length of the sample is much less than the radius of the heating beam. In these cases the thermal bump barely extends beyond the heating beam profile and follows the phase of the latter. This situation can be attained experimentally by using a high modulation frequency, or a large heating beam or a combination of both. If the phase distorsion introduced by a Gaussian surface is small, the resulting reflected beam can still be handled by Gaussian optics. This assumption obviates the need of a time-consuming diffraction calculation from the sample surface to the detector and permits us to explore the essential physics of the situation.

We will be making use of the complex representation of the Gaussian beam in the form of a modified spherical wave propagating in the positive z direction:

$$E(x,y,z,t) = E_0 \frac{-iz_0}{z - z_1 - iz_0} \exp ik\left[z + \frac{x^2 + y^2}{2(z - z_1 - iz_0)}\right] \quad , \tag{2}$$

where E_0 is the amplitude of the electric field, k is the optical wave number, the real constant z_0 defines the waist size w_0 (at $z = z_1$) through

$$z_0 = w_0^2 k/2 \quad . \tag{3}$$

Since this form can be derived from the following exact solution to the wave equation

$$E(x,y,z,t) = E_0 e^{ik\rho}/\rho \quad , \tag{4}$$

where

$$\rho = \sqrt{x^2 + y^2 + (z - z_1 - iz_0)^2} \quad , \tag{5}$$

by making expansions appropriate in the Fresnel regime ($x,y << |z-z_1-iz_0|$), it correctly describes the propagating behavior of a Gaussian beam. That is, if a light beam is known to be Gaussian at one position of z (i.e., its radial intensity and phase distributions are Gaussian) then by matching it with the expression (2) the characteristics of this beam at any other position of z is known. This is the basic technique we have used to avoid a diffraction calculation. In this analysis two important effects will be treated. The first is the phase change introduced by the sinusoidally moving reflecting sample surface (assuming normal incidence). The second is the slight intensity change caused by the sinusoidally varying reflectivity of the surface which, in turn, is a result of the modulated heating. The amplitude reflection coefficient of the sample surface will be modeled as

$$R(x,y,t) = R_0 + \delta R \cos(\Omega t + \theta_R) \exp[-(x^2+y^2)/r_b^2] \quad , \tag{6}$$

where R_0 is the amplitude reflection coefficient of the unheated sample surface and θ_R is the phase of the temperature variation. We have implicitly assumed that the modulated temperature distribution has the same Gaussian radius as the thermal bump in the same spirit of the earlier assumption. We introduce these effects into the calculation by the following multiplicative factor to the amplitude of the optical wave

$$R(x-x_1,y,t) \exp[-2ik\, h(x-x_1,y,t)] \quad , \tag{7}$$

where we have placed the center of the thermal bump at $x=x_1$, $y=0$. Keeping in mind the fact that the maximum height of a typical thermal bump is much less than 1Å, the quantity in the exponent in (7) is always much than unity. The following approximation is therefore valid.

$$\exp[-2ik\, h(x-x_1,y,t)] = 1 - 2ik\, h(x-x_1,y,t) \quad . \tag{8}$$

When a detector with a narrow slit along the y-direction is scanned in the x-direction, the received signal is the intensity of the reflected beam integrated along y-direction. In the integrated result there are dc terms, terms with frequency Ω and terms with frequency 2Ω. Only the terms with frequency Ω will be detected by the lock-in amplifier. They represent essentially the interference between the dc and the ac components of the beam and are linear in the small quantities δh and δR.

The final expression for the lock-in detected interference signal is quite lengthy and cumbersome, but it can be summerized simply as

$$\exp(a + rx + px^2) \cos(b + tx + sx^2) \quad , \tag{9}$$

with

$$a + ib = \frac{1}{2} \ln \frac{2\pi}{ik} + \ln (I_0 z_0^2) + \ln \frac{z_1' - iz_0'}{z_1 - iz_0} + \ln \left[\frac{\delta R}{R_0} \cos \theta_R - 2ik\, \delta h \cos \theta_h \right]$$

$$- \frac{1}{2} \ln \left\{ \left[(z_1' - z_1) - i(z_0' + z_0) \right] (z_1 + d + iz_0) (z_1' + d - iz_0') \right\}$$

$$- i \frac{kx_1^2}{2} \frac{\left[(z_1' - z_1) - i(z_0' - z_0) \right] (z_1 + d - iz_0)}{(z_1' + d - iz_0')(z_1 - iz_0)^2} \quad , \tag{10}$$

$$r + it = ikx_1 \frac{\left[(z_1' - z_1) - i(z_0' - z_0) \right]}{(z_1' + d - iz_0')(z_1 - iz_0)} \quad , \quad \text{and} \tag{11}$$

$$p + is = - \frac{ik}{2} \frac{\left[(z_1' - z_1) - i(z_0' + z_0) \right]}{(z_1' + d - iz_0')(z_1 + d + iz_0)} \quad , \tag{12}$$

where I_0 is the reflected beam intensity ($=R_0^2 E_0^2$), x_1 is the offset between the centers of the probe and heating beams, and d is the sample to detector distance. The constants z_0 and z_1 are the beam parameters of the probe beam as defined in (2). The constants z_0' and z_1' are the corresponding parameters of the ac beam which results from the diffraction from the thermal bump, they are related to z_0 and z_1 through a lens-like equation

$$\frac{1}{z_1' - iz_0'} - \frac{1}{z_1 - iz_0} = \frac{2i}{kr_b^2} \quad . \tag{13}$$

The constants a, b, r, t, p, and s can be obtained from a least-square fit to the measured dc beam intensity profile and the ac interference pattern. The unknown quantities δR, δh and r_b also emerge from the least-square fit. Note that the first two appear together only in the combination

$$\frac{\delta R}{R_0} \cos \theta_R - 2ik\, \delta h \cos \theta_h \quad . \tag{14}$$

Since θ_R and θ_h are measured relative to the phase setting of the lock-in amplifier, the quadrature signal of a vector lock-in amplifier gives the same result except that the cosine functions in Eq.(14) are replaced by sine functions. This permits both $\delta R/R_0$ and δh to be determined independently.

RESULTS

In order to verify the general correctness of the above phenomenological theory, we made several scans changing only the value of x_1. Figure 4 shows the result of such scans compared with the curves calculated from Eq. (9) with values of parameters determined by a least-square fit. The fit is not as good towards the shoulders of the beam. This is attributable to the same observed deviation of the profile of the dc beam from a perfect Gaussian distribution.

We have applied this interferometric technique to a silicon wafer which has a doped (with boron, to 10^{16} cm^{-2}) region. Figure 5 shows the resulting bump heights from both doped and undoped regions as a function of the modulation frequency.

CONCLUSIONS

We have reported a novel single beam interferometric technique which has quite good sensitivity. The main advantage of this method is its simplicity in experimental arrangement. A single unfocused laser beam is used and there is not a single optical component between the laser and the detector except the sample surface. It must be kept in mind, however, this method is

limited to samples whose surfaces are specular reflectors. Pending more theoretical development, this method should be very suitable to thin film materials. Because of the thermoelastic process involved in this kind of interferometry, it should be especially good in determining adhesion property of thin films to their substrates.

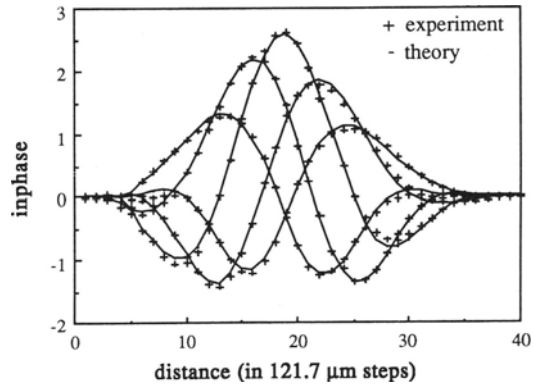

Fig. 4. Experimental data and the theoretical fit of the inphase signal, for five different heating beam positions within the probe beam.

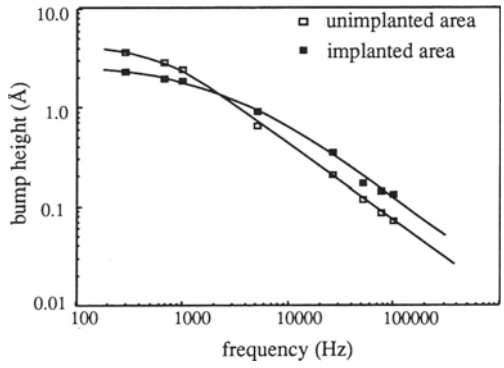

Fig. 5. Plot of bump height vs.frequency of the unimplanted region and a implanted region (50 kev B^+, 10^{16} ions/cm^2) of a p-type Si wafer.

ACKNOWLEDGEMENT

This work was sponsored by the Institute for Manufacturing Research, Wayne State University, Detroit, Michigan.

REFERENCES

1. A. Rosencwaig, J. Opsal, W.L. Smith, and D.L. Willenborg, J. Appl. Phys. **59**, 15 (1986).
2. J. Hartikainen, J. Jaarinen, and M. Luukkala, Can. J. Phys. **64**, 1341 (1986).
3. D. Royer and E. Dieulesaint, Appl. Phys. Lett., **49**, 1056, (1986).
4. H.K. Wickramasinghe, Y. Martin, D.A.H. Spear, E.A. Ash, J.Physique.Coll. C6, **44**, 191 (1983).
5. M.A. Olmstead, N.M. Amer, S.E. Kohan, D. Fournier, A.C. Boccara, Appl. Phys. A, **32**, 141 (1983).
6. L.D. Favro and M. Munidasa, in Reviwe of Progress in Quantitative NDE, Ed. D.O. Thompson and D.E. Chimenti, Vol 8 (to be published).